

# The effect of the Rossby number on vortex shedding and associated surface pressure drag in low Froude number flows

Jorge A. Gutiérrez<sup>1</sup>

*LLAP, CIGEFI, Escuela de Física, Universidad de Costa Rica*

(Received 11 may 1998, accepted 19 june 1998)

## ABSTRACT

The effect of the Rossby number in the shedding of vortices and the associated surface pressure drag is investigated. Four different case studies are analysed, namely,  $Ro=\infty$ ,  $Ro=0.2$ ,  $Ro=0.4$  and  $Ro=0.8$ . The flows investigated here are simulated by means of a three-dimensional numerical, non-hydrostatic, non-linear numerical model.

It is found that the shedding frequency increases with increasing Rossby number in the experiments which include background rotation. It is also found that vortex shedding leaves a trace in the surface pressure drag.

## 1. Introduction

The effect of mountains on atmospheric circulations is important. In the mesoscale the interaction of orography with the atmosphere may lead to :

- i) mountain wave generation
- ii) lee vortex formation and possibly to lee vortex shedding
- iii) cloud formation and orographic rain or orographic enhancement of rain
- iv) katabatic or anabatic winds
- v) clear air turbulence which presents a great hazard to aviation

- vi) modification of the path followed by pollutants
- vii) deformation of the boundary layer.

Large mountain ranges such as the Rocky mountains or the Tibetan plateau also affect the general circulation of the atmosphere by means of the generation of Rossby waves. They also act as elevated heat sources.

The orography can also induce gravity wave drag. The need to include the effect of the gravity wave drag produced by subgrid scale mountains was first suggested by Sawyer (1959). Bretherton (1969), evaluated the gravity wave drag in a particular case study and concluded that it could make an

---

<sup>1</sup> Corresponding author address: Dr Jorge A. Gutiérrez, Escuela de Física, Universidad de Costa Rica, 2060 San José, Costa Rica.  
E-mail: jgutier@ariel.efis.ucr.ac.cr

important contribution to the momentum balance of the large scale flow.

Vortex shedding can be produced in low Froude number flows when asymmetries are present in the flow, Sun and Chern (1994). In this paper it is intended to investigate the effect of the Rossby number on vortex shedding and the associated surface pressure drag by means of numerical simulations.

## 2. Numerical Model

The numerical model employed to investigate the impact of the Rossby number on vortex shedding is a three-dimensional, non-linear, non-hydrostatic model developed at the University of Reading by Pedro Miranda. A description of the model can be found in Gutiérrez (1997).

The model uses terrain-following  $\sigma$  (scale pressure) coordinates. The approximations to the model's equations are obtained by means of second-order centred finite differences. The variables are located on a staggered grid (Arakawa C-grid).

The model's equations are obtained as an approximation to the Navier-Stokes set of equations, written in terms of a reference state in hydrostatic equilibrium, which is a function of pressure only.

The boundary conditions imposed at the lateral boundaries and at the top of model domain are intended to minimise wave reflections at those boundaries. On the top of the model this is done by means of an absorption layer. Lateral boundary conditions are given by radiative boundary conditions.

The orography used is a bell-shaped mountain given by,

$$z(x,y) = \frac{h}{\left[1 + \left(\frac{x-x_0}{a}\right)^2 + \left(\frac{y-y_0}{b}\right)^2\right]^{\frac{3}{2}}} \quad (1)$$

where  $h$  is the height of the orography,  $a$  and  $b$  are the half-width lengths of the mountain and  $x_0$  and  $y_0$  are the coordinates of the centre of the orography. In all experiments presented here  $a = b$ , i.e., the

mountain has a circular base and  $h$  has been chosen to be equal to 2 kilometres. The model uses thirty vertical levels and unless stated otherwise the separation between consecutive grid points in both the zonal and meridional directions is equal to 15 kilometres.

### 3.1. Effects of the Rossby number on the shedding of vortices

The flows investigated in this paper have a Froude number equal to 0.2. Here the Froude number is defined as  $Fr = U/Nh$ , where  $U$  is the background speed of the flow,  $N$  is the Brunt-Väisälä frequency and  $h$  is the height of the obstacle.

Lee-vortex formation takes place in low Froude number flows, see for example, Smolarkiewicz and Rotunno (1989). Under certain circumstances (Sun and Chern, 1994, Gutiérrez and Thorpe 1997), lee vortices can be shed away from the orography.

Results of four different simulations will be shown and investigated. The Froude number, as mentioned above, shall remain constant throughout the simulations. The Rossby number  $Ro = U/fD$  is defined as the ratio between the background speed of the flow and the product of the Coriolis parameter by the diameter of the orography.

In order to keep the Froude number constant while varying the Rossby number the diameter of the mountain will be varied. The only departure from this procedure will be the case of an infinite Rossby number which corresponds to a simulation without background rotation, that is, the Coriolis parameter is nil.

### 3.2. First case study: flow without background rotation ( $Ro = \infty$ )

Consider the signal produced in the components of the drag by flow without background rotation. After a 72-hour simulation two counter-rotating vortices are formed on the lee of the obstacle. These vortices remain attached to the orography. Thus no vortex shedding takes place in this numerical experiment.

The dimensions of the orography are, height equal to 2 kilometres and base having a radius of 50 kilometres.

### 3.2.1. Drag

One measurable quantity that gives information about the overall flow is the drag force on the obstacle. Because of this some attention will be given to this quantity in order to investigate how it may help to detect if the lee vortices are shed away from the mountain.

When flow moves past a solid body, a force is exerted on the body by the fluid. Contributions to this total force are made by the tangential stress at the body surface (acting in the direction parallel to the surface of the body), integrated over that surface, and by the normal stress (acting perpendicular to the surface of the obstacle or barrier). The total force due to the tangential stresses will usually be approximately opposite in direction to the velocity of the fluid, and is termed 'friction drag' since it is wholly and directly a consequence of viscosity or internal friction in the fluid.

The total force due to the normal stress at the surface of an obstacle in the flow has a more complex origin, it results from differences of pressure over the surface of the body and is termed pressure drag. It is useful to recognise the following possible contributions to the pressure drag (Athanasiadou 1995):

The lift on the obstacle. This is a component of the total force normal to the direction of the motion, and is large for bodies of certain shape.

The induced drag. An accompaniment to the lift on a three-dimensional obstacle is the existence of vortices which trail downstream from the body. The obstacle continually supplies kinetic energy to the fluid as these trailing vortices increase in length, this energy being the manifestation of work done by the obstacle against that part of the total force known as induced drag.

The form drag. This is the component of the resultant force parallel (and opposite in direction) to the velocity of the fluid, after the induced drag has been subtracted. The form drag depends strongly on the shape of the obstacle.

For orographic flows, the body or obstacle corresponds to the mountain and the fluid to the atmosphere. The pressure drag force on the mountain is given by

$$\vec{D} = - \iint p_{surface} \vec{\nabla} h(x,y) dx dy \quad (2)$$

where,  $h(x,y)$  represents the orography and  $p_{surface}$  is the surface pressure. In the Reading model the surface pressure drag is calculated at regular intervals, generally every time step. The minus sign refers to the fact that it is the force acting on the atmosphere that is considered. Sometimes, the surface pressure drag associated with mountain ranges is also called mountain drag.

In geophysical flows, there are many mechanisms that can possibly contribute to pressure differences along the sides of a mountain and therefore to pressure drag. The responsible mechanisms are physically distinct but a combination can be possible depending on the scale of the mountain and the atmospheric conditions. Below, some possible mechanisms that would result in pressure differences on the mountain's surface and therefore pressure drag are described (Athanasiadou 1995):

- (a) Flow separation. In this case, buoyancy forces are not important. This is the primary mechanism of drag for the high Reynolds number flows around any object that is not carefully streamlined. The surface streamline leaves the mountain downstream of the crest, forming in effect a new broader shape including both the mountain and the separated region. The pressure just over the crest of the effective shape, which is equal to or slightly less than the free-stream static pressure, is transmitted through the the separated region to the lee side of the mountain. On the windward side of the mountain the pressure is higher than the free-stream static pressure due to a slowing of the flow there. The resulting

pressure drag force is quite sensitive to the shape of the mountain and the level of turbulence upstream.

- (b) Vertically propagating internal gravity waves. The generation of vertically propagating internal gravity waves can be an important drag mechanism for mountain flow. The fluid inertia is no longer the only cause of pressure differences since buoyancy forces become in this case important.
- (c) Trapped (resonant) internal gravity waves. This mechanism is similar to that discussed in (b), except that these shorter waves propagate horizontally along layers of large static stability and low wind speed in the lower troposphere. Like the generation of vertically propagating waves, this mechanism would be associated with stratified conditions, slow flow on the windward side and strong flow on the lee side of the mountain.

When the rotation of the Earth is included in the study of orographic flows there is an additional pressure force acting on the mountain due to the background pressure gradient associated with the mean flow. The mountain finds itself in a pressure field, and according to Archimedes' principle, experiences a force given by the mountain volume  $V_{mount}$ , times the background pressure gradient:

$$G = V_{mount} \nabla p = -V_{mount} (k \times \rho_0 f U_0) \quad (3)$$

where  $p$ ,  $\rho_0$  and  $\vec{U}_g$  are the mean horizontal pressure, mean density and mean geostrophic wind respectively. This force always acts at a right angle to the mean flow and for that reason is occasionally referred to as 'lift' force.

Flow-splitting, the tendency of the flow to move around the mountain rather than above it, occurs for low Froude number flows. This is also dependent on the shape of the obstacle. Smith (1980) found that this is due to the upstream pressure field causing stagnation on the upstream obstacle surface at a location given approximately by linear perturbation

theory. If upper-level overturning, as in the experiment of Crook et al. (1990), or lee-side separation forming a wake occur, both tend to promote flow-splitting; that is, cause it to occur at a larger Froude number than it would otherwise, by increasing the pressure on the upstream slope, but are not necessary for its occurrence. Conversely, as pointed out by Baines (1995), flow-splitting tends to promote lee-side separation and reduce upper-level overturning, since it involves more lateral flow around the obstacle.

The zonal and meridional components of the drag will be used to investigate if the shedding of vortices leaves a signal in the surface pressure drag.

The value of the zonal component of the surface pressure drag predicted by the linear hydrostatic

$$D_{linear} = -\frac{\pi}{4} \rho N U a h^2 \quad (4)$$

limit is given by

where  $\rho$  is the density of the fluid,  $N$  is the Brunt-Väisälä frequency,  $U$  is the background speed of the flow,  $a$  the half-width length of the mountain and  $h$  is the height of the obstacle.

Consider the signal produced in the components of the drag by flow without background rotation. After a 72-hour simulation two counter-rotating vortices are formed on the lee of the obstacle. These vortices remain attached to the orography. Thus no vortex shedding takes place in this numerical experiment.

The orography used in this simulations has a height of two kilometres and a base of 50 kilometres.

Figure 1 shows the results of a calculation of the zonal and meridional components of the surface pressure drag. The value of the zonal component of the surface pressure drag is found to be smaller than the magnitude predicted by the linear hydrostatic limit which is given by Equation (4).

$D_{linear} = -6.28 \times 10^9 N$ , the value of the zonal component of the drag, is about half the value given by the linear hydrostatic limit. This is easy to see

### Evolution of the surface pressure drag

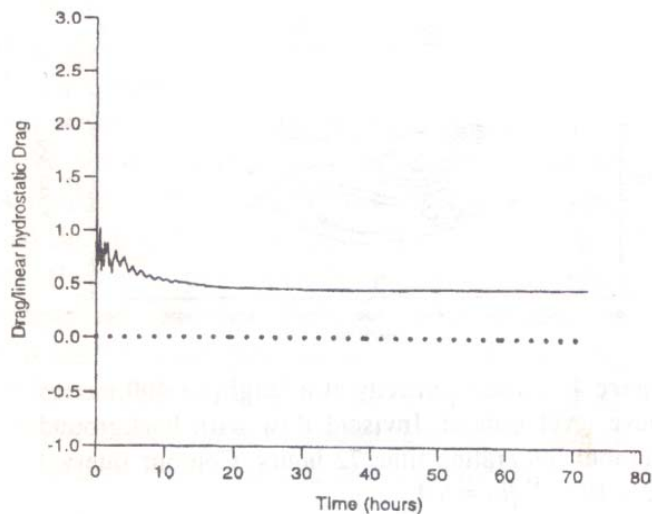


**Figure 1.** Evolution of the zonal component (continuous line) and the meridional component (broken line) of the surface pressure drag for the case of an isolated bell-shaped mountain. Integration time 72 hours. All values are normalised by the drag generated by the linear hydrostatic flow over the same mountain.

in Figure 1, where the values of the zonal and meridional components of the drag have been normalised by the drag of the linear hydrostatic flow over the same mountain. This is in agreement with the results of Miranda and James (1992, see their Figure 1). This is characteristic of the drag in low Froude number flows due to the small amplitude of the gravity waves. Larger values of the surface pressure drag are obtained in high Froude number flow regimes due to the increase of the amplitude of the gravity waves (Miranda and James 1992).

The meridional component of the drag, also known as the lift, is equal to zero. This is to be expected because of the absence of background rotation which results in symmetric flow with respect to a vertical plane passing through the centre of the orography. This renders impossible for the flow to develop pressure differences between the northern and southern slopes of the mountain. It is of interest in the study of lee vortices to see if the shedding of vortices leaves a signal in the meridional component of the drag due to the changes in the circulation of the flow around the orography when a vortex is advected downstream.

### 3.3. Second case study-Investigation of a flow whose Rossby number is equal to 0.2

Consider now a mountain with a height of 2 kilometres and a radius of 100 kilometres. The orography used is the same bell-shaped mountain employed in the first numerical experiment discussed in this article. The background speed of the wind and the stratification of the flow remain the same as in the experiment described in the first case study. The Froude number of the flow remains the same, that is, equal to 0.2. This is chosen to be so because the Froude number is the main parameter used in this article to investigate the shedding of vortices.

It can be observed in Figure 2 that the vorticity field at a height of 400 metres above level ground shows an important deflection towards the south of the mountain, indicating that background rotation has a more important impact on the structure of the mountain's wake than in the case of orographic features with smaller horizontal dimensions. Only two vortex centres have been shed in this case.

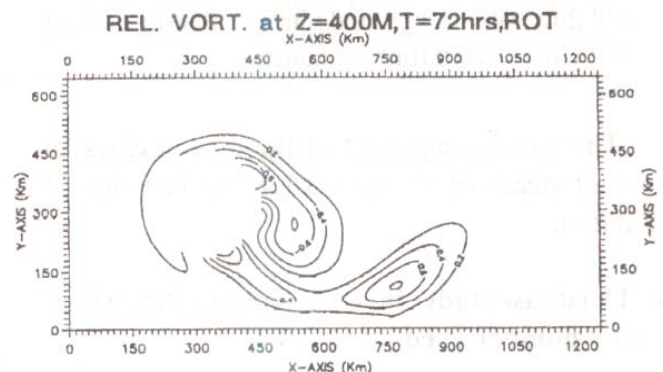


**Figure 2.** Vertical vorticity field for flow with Rossby number equal to 0.2 at a height of 400 metres above level ground. Contour interval  $0.2 \times 10^{-4} \text{ s}^{-1}$ . Inviscid flow with background rotation. Integration time 72 hours.

#### 3.3.1. Evolution of the drag

The evolution of the drag in this experiment is shown in Figure 3. Notice that the meridional component of the drag in this simulation reaches a local maximum at  $T=12$  hours of about  $-1.3 \times 10^{10} \text{ N}$ .

The time evolution of the meridional component of the drag shows two local maxima, after 12 and

38 hours of simulation, which indicates a link between the temporal behaviour of the meridional component of the drag and the shedding of lee vortices shown in Figure 3.

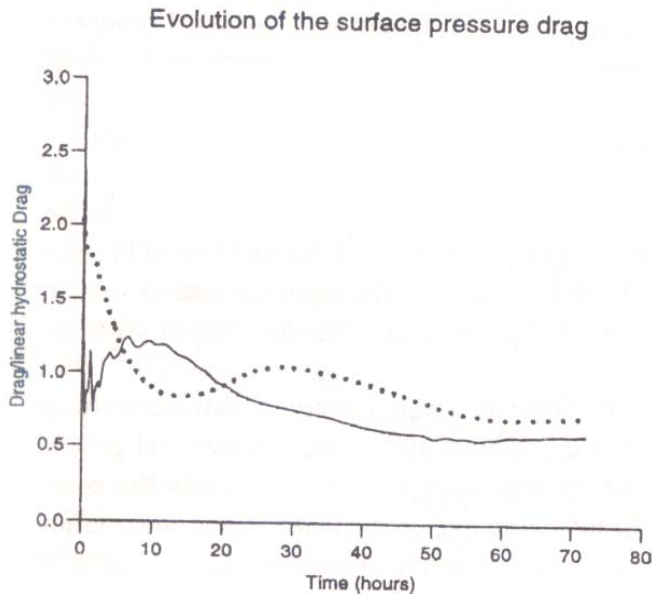


**Figure 3.** Evolution of the normalised zonal component (continuous line) and the normalised meridional component (dotted line) of the surface pressure drag. Inviscid flow with background rotation. Rossby number flow 0.2. Integration time 72 hours.

The zonal component of the drag reaches an apparent steady-state value after twenty hours of simulation.

### 3.4. Third case study- Investigation of a flow whose Rossby number is equal to 0.4

In this case the mountain remains having a height of 2 kilometres but its radius is now equal to 50 kilometres, i.e., half the size of the orography used in the experiment with  $Ro = 0.2$ . This means that the aspect ratio of the mountain,  $h/a$ , has increased by a factor of two. Here  $h$  is the height of the obstacle and  $a$  its radius. The Froude number of the flow remains equal to 0.2.

Figure 4 shows that after 72 hours of simulation three vortex centres have been shed from the orography, that is, the frequency of shedding has increased. Also there is a slight increase of about  $0.2 \times 10^{-4} s^{-1}$  in the vertical vorticity field.

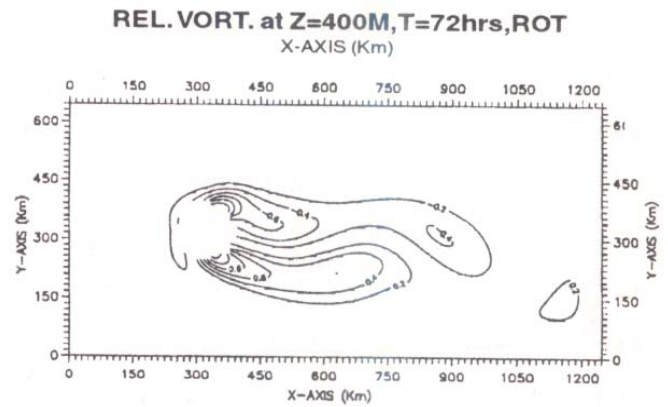


**Figure 4.** Vertical vorticity at a height of 400 metres above level ground. Inviscid flow with background rotation. Integration time 72 hours. Contour interval  $0.2 \times 10^{-4} s^{-1}$ ,  $Ro = 0.4$ .

In the present simulation neither the zonal nor the meridional components of the surface pressure drag are equal to zero. The zonal component of the drag, after some oscillations generated by the impulsive start up procedure evolves towards a steady regime.

The meridional component oscillates with a larger amplitude and two relative maxima can be observed in Figure 5. Recall that in the presence of background rotation a pressure difference develops between the southern and northern flanks of the

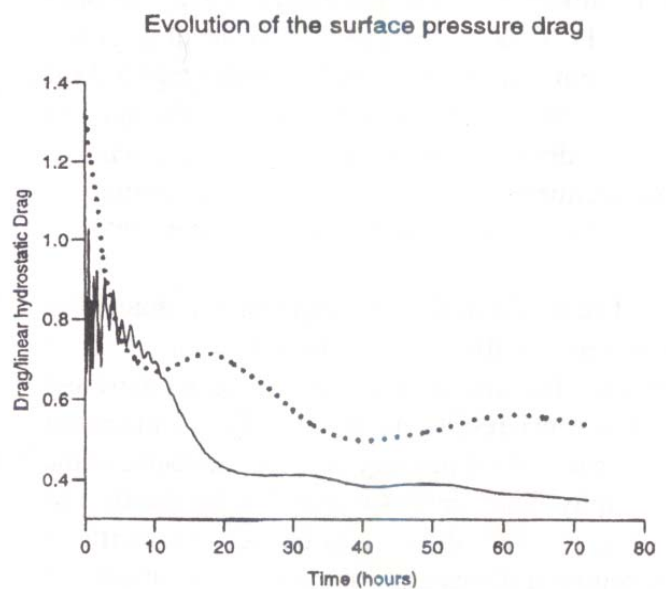


**Figure 5.** Evolution of the normalised zonal component (continuous line) and the normalised meridional component (dotted line) of the surface pressure drag. Inviscid flow with background rotation. The Rossby number of the flow is 0.4. Integration time 72 hours.

mentioned in this article. Thus the shedding of vortices does have an impact, even though it is a small one, on the pressure forces around the obstacle from which they are shed. This result can be seen in Figure 7.

**TABLE 1.** Data on Strouhal numbers corresponding to different Rossby number flows.

Rossby number	0.2	0.4	0.8
Strouhal number	0.45	0.34	0.14

Table 1 shows a summary of the results obtained for the simulations with background rotation performed with four different Rossby number regimes. It is found that the Strouhal number varies inversely with respect to the Rossby number. The non-dimensional frequency of vortex shedding given by the ratio  $S = \nu d / U$  is known as the Strouhal number, where  $\nu$  is the frequency at which vortices are shed from an obstacle,  $d$  is the diameter of the obstacle and  $U$  is the upstream value of the background velocity.

Looking at Table 1, one can see that the Strouhal number computed for the regimes with Rossby numbers 0.8 and 0.4 are within the range of Strouhal numbers found in the investigation of flow past the Aleutian islands displayed in Table 2. The value of the Strouhal number computed for the case of a Rossby number equal to 0.2 is found to be larger than those shown in Table 2.

**TABLE 2.** Data on islands from which vortex shedding is frequently observed, from Trischka, 1980. Where  $a$  is the distance between successively shed vortices and one side of the vortex street,  $u_i$  is the speed of the shed vortices,  $u_o$  is the upstream speed,  $d$  is the obstacle dimension used by reporting authors to calculate the Strouhal number.

Feature	$a$ (km)	$u_i / u_o$	$d$ (km)	$u_o$ ( $ms^{-1}$ )	$S$	$T$ (hours)
Cheju	111	0.76	28	9.2	0.19	4.4
Kiska	85	0.75	18	10.0	0.16	3.1
Pavlov	65	0.75	18	10.0	0.21	2.4
Programni	50	0.75	13	10.0	0.20	1.9
Shishaldin	75	0.75	32	10.0	0.32	2.8
Vsevidof	75	0.75	17	10.0	0.17	2.8

#### 4. Conclusions

The speed of propagation of the shed lee eddies is found to be less than that of the upstream flow, which agrees with observational data of atmospheric lee vortices and with laboratory experiments performed on low Froude number flows.

As expected, the frequency of shedding of lee vortices is found to increase when steeper obstacles are employed.

The shedding of vortices leaves a signal in the meridional component of the surface pressure drag.

The influence of background rotation in the form of a southern deviation of the shed eddies, in the case of westerly flow impinging on an isolated obstacle located on the northern hemisphere is felt more strongly in the case of wide obstacles than in obstacles with a shorter horizontal extension.

#### RESUMEN

Se investiga el efecto del número de Rossby en la producción de calles de vórtices y el arrastre en superficie asociado. Cuatro experimentos numéricos son analizados estos corresponden a  $R_o = \infty$ ,  $R_o = 0.2$ ,  $R_o = 0.4$  y  $R_o = 0.8$ . Los flujos aquí investigados son simulados por medio de un modelo numérico tridimensional, no lineal y no hidrostático.

Se encuentra que la frecuencia de advección de vórtices o número de Strouhal crece según aumenta el número de Rossby cuando hay rotación del sistema de coordenadas. Se encuentra también que la advección de vórtices deja su huella en el arrastre de la presión en superficie.

#### References

- Athanassiadou, M. 1995. Linear and non-linear mesoscale flow associated with the Alps. Ph.D. thesis, University of reading, United Kingdom, 248 pp.
- Baines, P.G. 1995. Topographic effects in stratified flows. Cambridge University Press, 482 pp.
- Bretherton, F.P. 1969. Momentum transport by gravity waves. Quarterly Journal R. Met. Soc., 95, 213-243.
- Crook, N., T. Clark, and M.W. Moncrieff. 1990. The Denver Cyclone. Part I: Generation in low Froude-number flow. Journal of the Atmospheric Sciences. 47(23), 2725-2742.
- Gutiérrez, J.A. 1997. Description of a mesoscale (limited area) numerical model. Tópicos Meteorológicos y Oceanográficos. 4(2), 97-108.

- Gutiérrez, J.A. and A. J. Thorpe. 1997. Low Froude number stratified flows interacting with an isolated obstacle. *Tópicos Meteorológicos y Oceanográficos*. 4(2). 109-128
- Miranda, P.M. and I.N. James. 1992. Non-linear three-dimensional effects on gravity wave drag: splitting flow and breaking waves. *Q.J.R. Meteorol. Soc.* 118, 1057-1081.
- Sawyer, J.S. 1959. The introduction of the effect of topography into methods of numerical forecasting. *Q.J.R. Meteorol. Soc.* 85,31-43.
- Smith, R.B. 1980. Linear theory of stratified hydrostatic flow past an isolated mountain. *Tellus*. 32, 348-364.
- Smolarkiewicz, P. and R. Rotunno. 1989. Low Froude number flow past three-dimensional obstacles. Part I: Barclinically generated lee-vortices. *Journal of the Atmospheric Sciences*. 46 (23), 1154-1164.
- Sun, W. and J. Chern. 1994. Numerical experiments of vortices in the wakes of large idealised mountains. *Journal of the Atmospheric Sciences*. 51(2),191-201.
- Trischka, J.W. 1980. Cone models of mountain peaks associated with atmospheric vortex streets. *Tellus*. 32, 365-375.